GEOPHYSICS, VOL. 75, NO. 2 (MARCH-APRIL 2010); P. T37–T47, 7 FIGS.
10.1190/1.3346064

The velocity of energy through a dissipative medium

José M. Carcione[1], Davide Gei[1], and Sven Treitel[2]

ABSTRACT

The velocity of seismic and electromagnetic signals depends on properties such as elastic moduli, density, porosity, viscosity, dielectric permittivity, and conductivity. Hence, the identification of the correct velocity of energy transport is essential to obtain the characteristics of the medium. The energy and group velocities, defined for a monochromatic plane wave, are compared to the centrovelocity, related to the centroid of the pulse in the time and spatial domains. The comparison is performed for a 1D medium and a band-limited pulse with a given dominant frequency and taking into account that the centroid of the spectrum decreases with increasing distance. For a lossless medium, the three velocities coincide. In absorbing media, the centrovelocity is closer to the group velocity at short travel distances, in which the wave packet retains its shape. At a given distance, the centrovelocity equals the energy velocity, and beyond that distance this velocity becomes a better approximation. This is generally the case for the propagation of acoustic and electromagnetic waves in earth materials. In other cases, such as electromagnetic propagation at the atomic scale (Lorentz model), the meaning of the energy velocity needs to be revisited, and concepts such as the signal velocity are required.

INTRODUCTION

The velocity of a pulse in an absorbing and dispersive medium is a matter of controversy. The concept, which is relevant in the physics of materials and earth sciences, has been actively studied under the impetus provided by the atomic theory on the one hand, and by radio and sound on the other (Eckart, 1948). In seismology, the concept of velocity is very important because it provides the spatial location of an earthquake hypocenter and geologic strata (Ben-Menahem and Singh, 1981). Similarly, ground-penetrating radar applications are based on the interpretation of radargrams, whereby the traveltimes of the reflection events provide information about the dielectric permittivity and ionic conductivity of the shallow geologic layers (Carcione, 1996; Daniels, 1996).

Both descriptions of media, that is, seismic and electromagnetic media used in seismology and seismic prospecting, imply the absorption and dispersion of the acoustic and electromagnetic pulses. Traveltimes of seismic events are generally obtained from the onset of the pulse or its maximum amplitude. If the source-receiver distance is known, useful information about the medium properties can be inferred from the traveltime. This is done by using wave-velocity concepts whose expressions are explicit functions of those properties. Therefore, the identification of the best physical measure of velocity is essential.

The various velocities are strictly defined for a plane monochromatic wave, although they can be used also for quasi-monochromatic waves. In isotropic media, the energy velocity, obtained from Umov-Poynting's theorem, is equal to the phase velocity (Buchen, 1971; Borcherdt, 1973; Mainardi, 1973, 1987; Carcione, 2007); i.e., it is equal to the angular frequency divided by the wavenumber. The group velocity, obtained by the method of stationary phase (e.g., Eckart, 1948), is the derivative of the angular frequency with respect to the wavenumber. Carcione (1994) and Carcione et al. (1996) show that, generally, the concept of seismic group velocity as the velocity of the energy is lost in the presence of high attenuation (quality factors approximately less than 5). Sommerfeld and Brillouin (Brillouin, 1960) clearly show the breakdown of the group-velocity concept, which might exceed the velocity of light in vacuum and even become negative. They introduced the concept of signal velocity, which has been defined for the Lorentz model, but a general definition is still an open problem.

We note that in a general 3D medium (anisotropic and absorbing), there are four different velocities corresponding to a time-harmonic plane wave. They are the phase, energy, group, and envelope velocities (e.g., Carcione, 2007). The envelope velocity is a geometric concept (Postma, 1955) and is very close to the energy velocity in practice (Carcione, 1994, 2007). All of the velocities coincide for a lossless and isotropic medium. For a lossless and anisotropic medium, the envelope, energy, and group velocities coincide and differ from

Manuscript received by the Editor 7 July 2009; published online 23 March 2010.
[1]Istituto Nazionale di Oceanografia e di Geofisica Sperimentale, Trieste, Italy. E-mail: jcarcione@ogs.trieste.it, dgei@inogs.it.
[2]Tridekon, Inc., Tulsa, Oklahoma, U.S.A. E-mail: streitel@tridekon.net.

the phase velocity. For an absorbing and isotropic medium and homogeneous body waves, the phase, energy, and envelope velocities coincide and differ from the group velocity. When there is no loss, the energy velocity is identical to the group velocity, even if the medium is dispersive (Felsen and Marcuvitz, 1973; Mainardi, 1987).

For nonperiodic (nonmonochromatic) waves with finite energy, the concept of centrovelocity has been introduced (Vainshtein, 1957; Smith, 1970; Gurwich, 2001). Smith (1970) defines the centrovelocity as the distance traveled divided by the centroid of the time pulse. Van Groesen and Mainardi (1989), Derks and Van Groesen (1992), and Gurwich (2001) define the centrovelocity as the velocity of the "mass" center, where the integration is done over the spatial variable instead of the time variable, that is, on the snapshot of the wavefield instead of the pulse time history. Carcione et al. (1996) use a similar method to obtain the location of the energy in anisotropic anelastic media.

Van Groesen and Mainardi (1989) show that their centrovelocity differs from the energy velocity by a term that is due to the presence of dissipation (1D homogeneous media). They obtain explicit relations for the Korteweg-de Vries-Burgers and Klein-Gordon differential equations. However, unlike the phase (or energy) and group velocities, the centrovelocity depends on the shape of the pulse, which changes with time and travel distance. Therefore, an explicit analytic expression in terms of the medium properties alone cannot be obtained, even for a homogeneous medium. Bloch (1977) introduced another velocity, obtained from the crosscorrelation between the initial pulse and the propagating pulse, which seems to give satisfactory results when the pulse distortion is not very significant.

The concept of signal velocity introduced by Sommerfeld and Brillouin (Brillouin, 1960; Mainardi, 1983) describes the velocity of energy transport for the Lorentz model. It is equal to the group velocity in regions of dispersion without attenuation (Felsen and Marcuvitz, 1973; Mainardi, 1987; Oughstun and Sherman, 1994). There is theoretical evidence that the group velocity exceeds the velocity of light in vacuum (superluminal wave propagation) when a pulse propagates through a strongly dispersive medium determined by two spectral lines (Garrett and McCumber, 1970; Chiao, 1993). However, this does not mean that information can be transmitted at superluminal velocities, which implies the violation of causality.

Recently, Wang et al. (2000) reported a large superluminal effect for laser pulses of visible light, in which a pulse propagates with a negative group velocity. Basically, the conditions imply that the group velocity remains constant over the pulse bandwidth, so that the light pulse maintains its shape during propagation (Steinberg and Chiao, 1994). Such a situation can be obtained with an inverted medium possessing a doublet line. An example is the doublets occurring in alkali-metal atoms, split by the several-GHz ground-state hyperfine splitting. The theory describing the phenomenon of dispersion under these conditions involves two Lorentz models with inverted atomic populations (Steinberg and Chiao, 1994). However, the classical concepts of phase, energy, and group velocities break down for the Lorentz model, depending on the value of the source peak frequency and source bandwidth compared to the width of the spectral line.

To clarify the concept of wave velocity in the presence of attenuation, we consider a 1D medium and compare the energy (phase) and group velocities of a monochromatic wave to the velocity obtained as the distance divided by the traveltime of the centroid of the energy, where by energy we mean the square of the absolute value of the pulse time history. This concept is similar to the centrovelocity introduced by Smith (1970), in the sense that it is obtained in the time domain. Smith's definition is an instantaneous centrovelocity, as well as the Gurwich velocity (Gurwich, 2001), which is defined in the space domain.

The traveltimes corresponding to the "theoretical" energy and group velocities are evaluated by taking into account that the pulse peak frequency decreases with increasing travel distance. Thus, the peak frequency depends on the spatial variable and is obtained as the centroid of the power spectrum. A similar procedure is performed in the spatial domain by computing a centroid wavenumber. We consider several attenuation theories, namely, the Zener and constant-Q models of acoustics, and the Debye, ionic-conductivity, and Lorentz models of electromagnetism. The case of a single Lorentz model for resonance attenuation is controversial. The latter is not used in earth sciences applications, but provides an extreme case wherein the different velocities cannot describe the location of the pulse. In this case, the concept of signal velocity (Brillouin, 1960) and an energy-velocity expression proposed by Loudon (1970) seem to provide a satisfactory description of the pulse dynamics (Oughstun and Sherman, 1994).

ENERGY AND GROUP VELOCITIES

Waves are necessarily homogeneous in 1D space; i.e., the wavenumber-vector direction coincides with the attenuation-vector direction. Hence, the energy velocity is equal to the phase velocity (Ben-Menahem and Singh, 1981; Carcione, 2007). The energy velocity is given by

$$v_e(\omega) = \left[\mathrm{Re}\left(\frac{1}{v}\right)\right]^{-1} \tag{1}$$

(e.g., Carcione, 2007), where v is the complex velocity.

On the other hand, the group velocity is

$$v_g(\omega) = \left[\mathrm{Re}\left(\frac{dk}{d\omega}\right)\right]^{-1} = \left[\mathrm{Re}\left(\frac{a}{v}\right)\right]^{-1}, \tag{2}$$

where k is the complex wavenumber, ω is the angular frequency, and

$$a = 1 - \frac{\omega}{v}\frac{dv}{d\omega} \tag{3}$$

(Ben-Menahem and Singh, 1981; Carcione, 2007). In general, v and a are complex and frequency dependent. The complex wavenumber is

$$k = \frac{\omega}{v} = \kappa - i\alpha, \tag{4}$$

where κ is the real wavenumber and α is the attenuation factor, given by

$$\alpha = -\omega\,\mathrm{Im}\left(\frac{1}{v}\right). \tag{5}$$

The viscoelastic complex velocity is

$$v = \sqrt{\frac{M}{\rho}}, \tag{6}$$

where M is the complex modulus and ρ is the mass density. The electromagnetic complex velocity is

$$v = \frac{1}{\sqrt{\mu \epsilon^*}}, \quad (7)$$

where ϵ^* is the complex dielectric permittivity and μ is the magnetic permeability. By virtue of mathematical analogies (Carcione and Cavallini, 1995; Carcione and Robinson, 2002), M and ρ are mathematically equivalent to $1/\epsilon^*$ and μ, respectively.

The complex modulus M and dielectric permittivity ϵ^* of the different attenuation models analyzed in the following sections are described in Appendix A.

GREEN'S FUNCTION AND TRANSIENT SOLUTION

The 1D Green's function (impulse response) of the medium is

$$G(\omega) = \exp(-ikx) \quad (8)$$

(e.g., Eckart, 1948), where x is the travel distance.

We consider that the time history of the source is

$$f(t) = \left(\beta - \frac{1}{2}\right)\exp(-\beta), \quad \beta = \left[\frac{\pi(t-t_0)}{t_p}\right]^2, \quad (9)$$

where t_p is the period of the wave (the distance between the side peaks is $\sqrt{6}t_p/\pi$), and $t_0 = 1.5t_p$ is a delay time. Its frequency spectrum is

$$F(\omega) = \left(\frac{t_p}{\sqrt{\pi}}\right)\bar{\beta}\exp(-\bar{\beta} - i\omega t_0), \quad \bar{\beta} = \left(\frac{\omega}{\omega_p}\right)^2, \quad (10)$$

$$\omega_p = \frac{2\pi}{t_p}.$$

The peak frequency is $f_p = 1/t_p$.

Then the frequency-domain response is

$$U(\omega) = F(\omega)G(\omega) = F(\omega)\exp(-ikx), \quad (11)$$

and its power spectrum is

$$P(\omega) = |U(\omega)|^2 = \left(\frac{t_p^2}{\pi}\right)\bar{\beta}^2\exp[-2(\alpha x + \bar{\beta})], \quad (12)$$

where we have used equation 4 and α is given by equation 5. A numerical inversion by the discrete Fourier transform yields the desired time-domain (transient) solution.

NUMERICAL EVALUATION OF THE VELOCITY OF THE ENERGY

In this section, we obtain expressions of the energy and group velocities and two centrovelocities (i.e., computed with the centroid concept) (Smith, 1970; Gurwich, 2001). Note that the centroid frequency is not necessarily equal to the peak frequency of the source. This is always true for the pulse given in equation 9 because the spectrum is not symmetrical with respect to the peak frequency.

The energy of a signal is defined as

$$E = \int_0^\infty |u(t)|^2 dt = \frac{1}{2\pi}\int_{-\infty}^\infty |U(\omega)|^2 d\omega, \quad (13)$$

where $u(t)$ is the Fourier transform of $U(\omega)$, and Parseval's theorem has been used (Bracewell, 1965).

We define "location of the energy" as the time t_c corresponding to the centroid of the function $|u|^2$ in the time domain (time history) (Bracewell, 1965). That is

$$t_c(x) = \frac{\int_0^\infty t|u(x,t)|^2 dt}{\int_0^\infty |u(x,t)|^2 dt}. \quad (14)$$

Then, the first centrovelocity, defined here as the mean velocity from 0 to x, is

$$\bar{c}_1(x) = \frac{x}{t_c(x)}. \quad (15)$$

The Smith centrovelocity is

$$c_1(x) = \left(\frac{dt_c(x)}{dx}\right)^{-1} \quad (16)$$

(Smith, 1970).

On the other hand, the energy and group velocities 1 and 2 are evaluated at the centroid ω_c of the power spectrum. Because the medium is lossy, frequency ω_c depends on the position x', where $0 \le x' \le x$. We have

$$\omega_c(x') = \frac{\int_0^\infty \omega P(\omega,x')d\omega}{\int_0^\infty P(\omega,x')d\omega} = \frac{\int_0^\infty \omega|F|^2\exp(-2\alpha x')d\omega}{\int_0^\infty |F|^2\exp(-2\alpha x')d\omega}, \quad (17)$$

where we have used equations 11 and 12.

The energy and group traveltimes then are obtained as

$$t_e(x) = \int_0^x \frac{dx'}{v_e[\omega_c(x')]}, \quad \text{and } t_g(x) = \int_0^x \frac{dx'}{v_g[\omega_c(x')]}, \quad (18)$$

and the respective mean velocities are

$$\bar{v}_e(x) = \frac{x}{t_e(x)} \quad \text{and } \bar{v}_g(x) = \frac{x}{t_g(x)}. \quad (19)$$

We define a second centrovelocity as the mean velocity computed from the snapshots of the field, from 0 to time t,

$$\bar{c}_2(t) = \frac{x_c(t)}{t}, \qquad (20)$$

where the location of the energy is

$$x_c(t) = \frac{\int_0^\infty x|u(x,t)|^2 dx}{\int_0^\infty |u(x,t)|^2 dx}, \qquad (21)$$

i.e., the centroid of the function $|u|^2$ in the space domain (snapshot). The Gurwich centrovelocity is

$$c_2(t) = \frac{dx_c(t)}{dt}. \qquad (22)$$

In this case, it is possible to compute the energy and group velocities if we assume a complex frequency $\Omega = \omega + i\omega_I$ and a real wavenumber κ. The dispersion relation is obtained from equation 6 if we consider a complex velocity equal to Ω/κ; that is, the dispersion relation is

$$\frac{\Omega}{\kappa} = \sqrt{\frac{M(\Omega)}{\rho}}. \qquad (23)$$

Generally, this equation has to be solved numerically for Ω to obtain $\omega(\kappa) = \mathrm{Re}(\Omega)$. Then the energy and group velocities are evaluated at the centroid κ_c of the spatial power spectrum. The centroid wavenumber κ_c depends on the snapshot time t', where $0 \le t' \le t$. We have

$$\kappa_c(t') = \frac{\int_0^\infty \kappa P(\kappa,t') d\kappa}{\int_0^\infty P(\kappa,t') d\kappa}, \qquad (24)$$

where $P(\kappa,t')$ is the spatial power spectrum obtained by an inverse spatial Fourier transform. The phase, energy, and group locations then are obtained as

$$x_p(t) = \int_0^t \frac{dt'}{v_p[\omega(\kappa_c(t'))]},$$

$$x_e(t) = \int_0^t \frac{dt'}{v_e[\omega(\kappa_c(t'))]},$$

and

$$x_g(t) = \int_0^t \frac{dt'}{v_g[\omega(\kappa_c(t'))]}, \qquad (25)$$

where

$$v_p[\omega(\kappa)] = \frac{\omega(\kappa)}{\kappa} = \mathrm{Re}(v), \quad v_e[\omega(\kappa)] = \left[\mathrm{Re}\left(\frac{1}{v}\right)\right]^{-1},$$

$$v_g[\omega(\kappa)] = \frac{\partial \omega(\kappa)}{\partial \kappa} = \mathrm{Re}\left[\frac{\partial \Omega(\kappa)}{\partial \kappa}\right]. \qquad (26)$$

Unlike the case of complex wavenumbers, an energy velocity that differs from the phase velocity arises from the energy balance (see Appendix B).

The respective mean velocities are

$$\bar{v}_p(t) = \frac{x_p(t)}{t}, \quad \bar{v}_e(t) = \frac{x_e(t)}{t}, \quad \text{and } \bar{v}_g(t) = \frac{x_g(t)}{t}. \qquad (27)$$

SIMULATIONS

We first define the properties of the attenuation models. The Zener model has $\omega_0 = 157/\mathrm{s}$ and $M_\infty = \rho c_\infty^2$, with $c_\infty = 2$ km/s. The Debye and ionic-conductivity models have $\omega_0 = 628/\mu\mathrm{s}$ $[f_0 = \omega_0/(2\pi) = 100$ MHz$]$ and $\epsilon_\infty = \mu^{-1} c_\infty^{-2}$, with $c_\infty = 29.9$ cm/ns, with $\sigma = \epsilon_\infty \omega_0 / Q_0$ for the second model. The constant-Q model has $\omega_0 = 157$ Hz and $M_0 = \rho c_0^2$, with $c_0 = 2$ km/s. The values of Q_0 are given below. (The values of the density and magnetic permeability are irrelevant for the calculations.)

Regarding the Lorentz model, a typical spectral-line example possessing a single ultraviolet resonance frequency has the following parameters: $\omega_0 = 4 \times 10^{16}/\mathrm{s} = 40\ \mathrm{fs}^{-1}$, $b^2 = 20 \times 10^{32}/\mathrm{s}^2$, and $\delta = 0.28 \times 10^{16}/s = 2.8\ \mathrm{fs}^{-1}$ (Oughstun and Sherman, 1994), where fs represents femtoseconds (1 fs $= 10^{-15}$ s). These values were chosen by Brillouin (1960) in his analysis of light-wave propagation.

We first consider the Zener model and illustrate the propagation effects. Figure 1 shows (a) the energy and group velocities as a function of frequency, (b) the initial spectrum (dashed line) and the spectrum at $x = 50$ m (solid line), and (c) the absolute value of the pulse in a lossless medium (dashed line) and for $Q_0 = 5$ (solid line) (in this case, the travel distance is $x = 1$ km). The group velocity is greater than the energy (phase) velocity. The amplitude of the spectrum for $Q_0 = 5$ is much lower than that of the initial spectrum, and the peak frequency has decreased. In Figure 1c, we might roughly estimate the pulse velocity by taking the ratio travel distance (1 km) to arrival time of the maximum amplitude. This gives 2 km/s (1 km/0.5 s) for $Q_0 = \infty$ (dashed-line pulse) and 1.67 km/s (1 km/0.6 s) for $Q_0 = 5$. More precise values are obtained in the following by using the centrovelocity.

The comparison between the energy and group velocities to the centrovelocities $\bar{c}_1$ and $\bar{c}_2$ (equations 15 and 20, respectively) is shown in Figure 2. In this case, $Q_0 = 10$. The relaxation mechanism has a peak at $f_0 = 25$ Hz, and Figure 2a and b correspond to source (initial) peak frequencies of 50 Hz and 25 Hz, respectively. As can be seen, the first centrovelocity is closer to the group velocity at short travel distances, where the wave packet maintains its shape. At a given distance, the first centrovelocity equals the energy velocity, and beyond that distance this velocity becomes a better approximation, particularly when the initial source central frequency is close to the peak frequency of the relaxation mechanism (the case of Figure 2b).

Let us consider the Debye model. Figure 3 shows (a) the energy (solid line) and group (dashed line) velocities as a function of frequency, (b) the time pulse for a travel distance $x = 30$ m, and (c) the first and second centrovelocities (dotted and dash-dotted lines, respectively) compared to the energy (solid line) and group (dashed line) velocities, as a function of travel distance. The minimum quality factor of the Debye peak is $Q_0 = 5$, and the source (initial) central frequency is twice the Debye relaxation frequency. The group velocity exceeds the velocity of light in vacuum (29.9 cm/ns) for a certain range of frequencies, whereas the energy velocity always is less than the velocity of light.

The results for the ionic-conductivity model are displayed in Figure 4. This figure shows (a) the energy and group velocities, and (b) the quality factor, as a function of frequency; (c) the magnetic field at three locations versus propagation time; and (d) the velocities as a function of distance. As before, the group velocity exceeds the velocity of light. The velocity vanishes at the low-frequency limit, and the attenuation factor α is constant for nonzero frequencies. In this case, the group velocity is also a good approximation because the pulse maintains its shape.

Figure 5 corresponds to the constant-Q model with $Q_0 = 5$. It shows (a) the energy (solid line) and group (dashed line) velocities as a function of frequency; (b) the pulse for a travel distance $x = 4$ km; and (c) the first (dotted line) and second (dash-dotted line) centrovelocities compared to the energy (solid line) and group (dashed line) velocities, as a function of travel distance. The source (initial) peak frequency is $f_p = 50$ Hz.

The velocities for the constant-Q model can be obtained analytically when the frequency is complex. The complex frequency is

$$\Omega(\kappa) = \omega_0 \left(\frac{\kappa}{\kappa_0} \right)^{1/(1-\gamma)} i^{\gamma/(1-\gamma)}, \quad \kappa_0 = \frac{\omega_0}{c_0}, \tag{28}$$

and we obtain

$$v_p(\kappa) = c_0 \left(\frac{\kappa}{\kappa_0} \right)^{\gamma/(1-\gamma)} \cos\left[\frac{\pi \gamma}{2(1-\gamma)} \right], \tag{29}$$

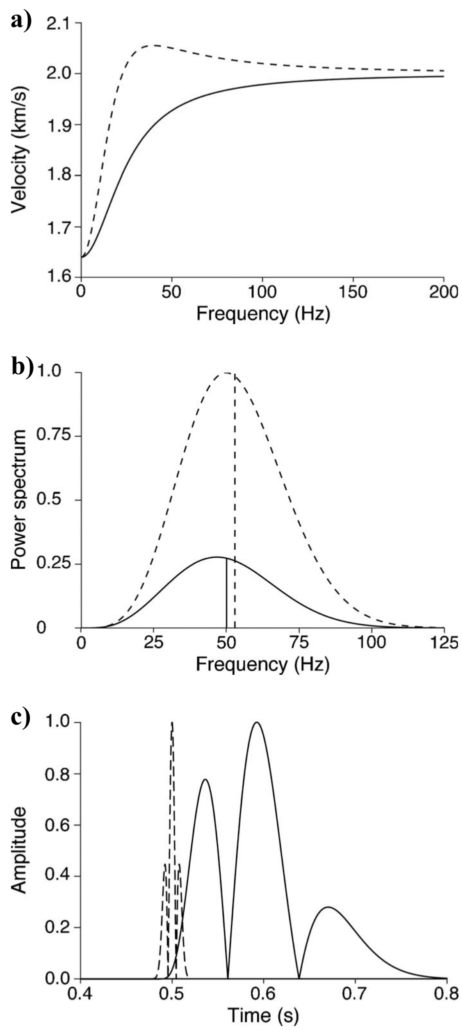

Figure 1. Zener model. (a) Energy (solid line) and group (dashed line) velocities as a function of frequency for $Q_0 = 5$. (b) Initial spectrum (dashed line) and spectrum for $x = 50$ m (solid line) (the solid and dashed vertical lines indicate the centroids.) (c) Pulse (absolute value of the normalized displacement) in a lossless medium (dashed line) and pulse for $Q_0 = 5$ (solid line) (the travel distance is $x = 1$ km). The relation between the pulse maximum amplitudes is 1.7×10^{-3}. The relaxation mechanism peaks at $\omega_0 = 157$/s ($f_0 = \omega_0/2\pi = 25$ Hz), and the source (initial) peak frequency is $\omega_p = 628$/s ($f_p = \omega_p/2\pi = 50$ Hz).

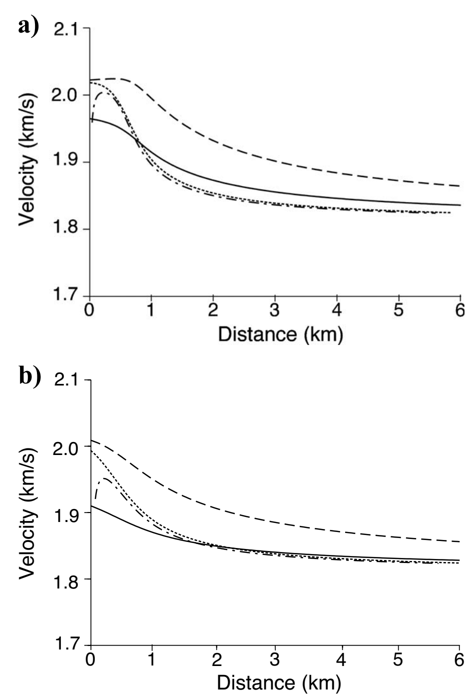

Figure 2. Zener model. First centrovelocity (dotted line), second centrovelocity (dash-dotted line), and energy (solid line) and group (dashed line) velocities as a function of travel distance and $Q_0 = 10$. The relaxation mechanism peaks at $f_0 = 25$ Hz, and the source (initial) peak frequency is (a) $f_p = 50$ Hz and (b) $f_p = 25$ Hz.

$$v_{\mathrm{e}}(\kappa) = v_{\mathrm{p}}(\kappa)\cos^{-2}\left[\frac{\pi\gamma}{2(1-\gamma)}\right], \tag{30}$$

and

$$v_{\mathrm{g}}(\kappa) = \frac{v_{\mathrm{p}}(\kappa)}{1-\gamma}. \tag{31}$$

Next, we compute the centrovelocity in the space domain, corresponding to the constant-Q model. Figure 6a shows the Gurwich centrovelocity (dotted line), the Smith centrovelocity (dash-dotted line), and the energy and group velocities (solid and dashed lines, respectively) as a function of travel distance, according to equations 22, 16, and 19, respectively. Figure 6b shows the propagating pulse

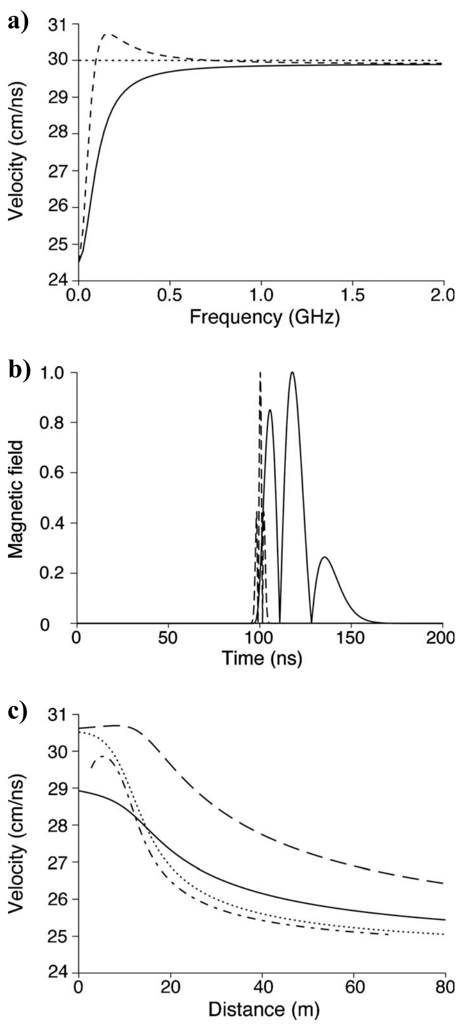

Figure 3. Debye model. (a) Energy (solid line), group (dashed line), and light (dotted line) velocities as a function of frequency, for $Q_0 = 5$. (b) Pulse (absolute value of the normalized magnetic field) in a lossless medium (dashed line) and pulse for $Q_0 = 5$ (solid line) for a travel distance $x = 30$ m. (c) First centrovelocity (dotted line), second centrovelocity (dash-dotted line), and energy (solid line) and group (dashed line) velocities as a function of travel distance for $Q_0 = 5$. The source (initial) peak frequency is $\omega_p = 1256/\mu\mathrm{s}$ [$f_p = \omega_p/(2\pi) = 200$ MHz], and the Debye mechanism has a peak at $f_0 = 100$ MHz.

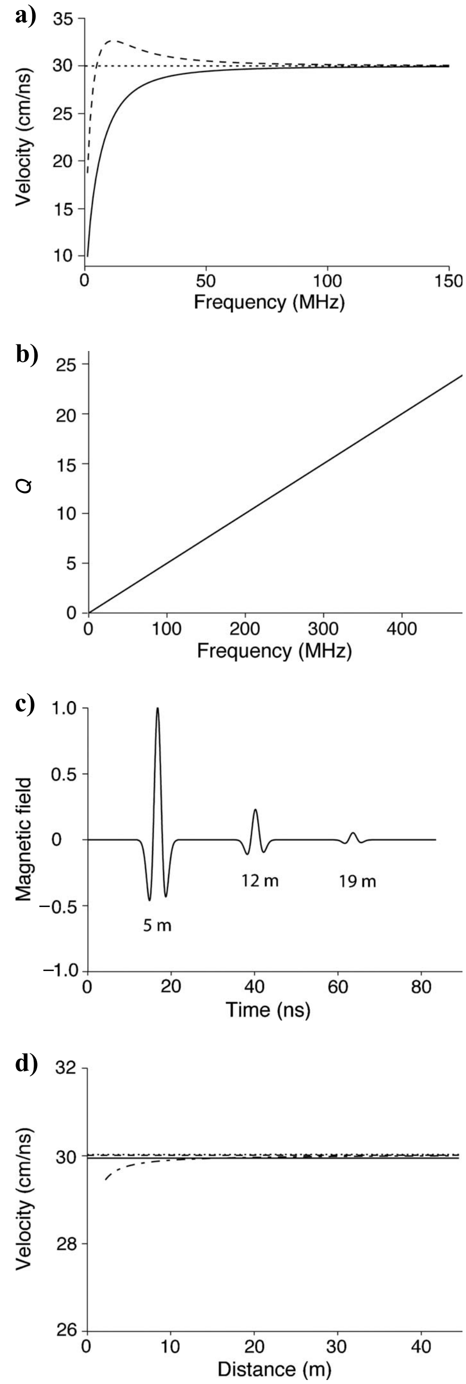

Figure 4. Ionic-conductivity model. (a) Energy (solid line) and group (dashed line) and light (dotted line) velocities, (b) quality factor as a function of frequency, (c) magnetic field at three locations versus propagation time, and (d) velocities as a function of travel distance: first centrovelocity (dotted line), second centrovelocity (dash-dotted line), and energy and group velocities (solid and dashed lines, respectively). The source (initial) peak frequency is $\omega_p = 1256/\mathrm{ns}$ [$f_p = \omega_p/(2\pi) = 200$ MHz]. The conductivity is $\sigma = \varepsilon_\infty \omega_p / Q_0$, where $Q_0 = 10$; i.e., $Q = 10$ at 200 MHz.

in the space-time domain. The time and space centroids (white dotted and dashed lines) are computed along the vertical and horizontal directions, respectively. The relaxation mechanism has a peak at $f_0 = 25$ Hz, $Q_0 = 5$, and the source (initial) peak frequency is $f_p = 50$ Hz. The two centrovelocities are slightly different, and this difference increases for increasing attenuation.

Finally, we display the velocities corresponding to the Lorentz model in Figure 7. The solid, dashed, and dotted lines are the energy, Loudon, and group velocities, respectively. The latter has two singularities and takes negative values, and the classical energy velocity exceeds the velocity of light. The Loudon velocity is well behaved because it is not negative and does not exceed the velocity of light. The group and Loudon velocities coincide outside the absorption region, in agreement with the fact that for a lossless but dispersive medium the energy and group velocities should be the same (Felsen and Marcuvitz, 1973; Mainardi, 1987). An analysis of the centrovelocities for this kind of model, representing a nonearth material, is outside the scope of this work. We represent the velocities to show that, for certain cases, even the energy velocity can have an unphysical behavior by exceeding the velocity of light. A different type of energy balance is required in these cases (e.g., Oughstun and Sherman, 1994).

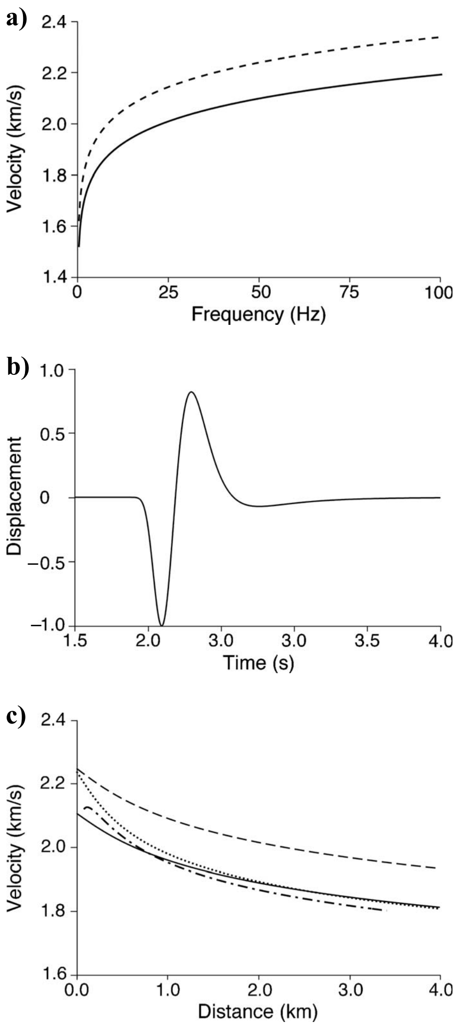

Figure 5. Constant-Q model. (a) Energy (solid line) and group (dashed line) velocities as a function of frequency; (b) pulse (normalized displacement) for a travel distance $x = 4$ km; and (c) first centrovelocity (dotted line), second centrovelocity (dash-dotted line), and energy and group velocities (solid and dashed lines, respectively). The source (initial) peak frequency is $\omega_p = 314/\mathrm{s}$ $[f_p = \omega_p/(2\pi) = 50$ Hz$]$ and $Q_0 = 5$. The relaxation mechanism has the peak at $f_0 = 25$ Hz.

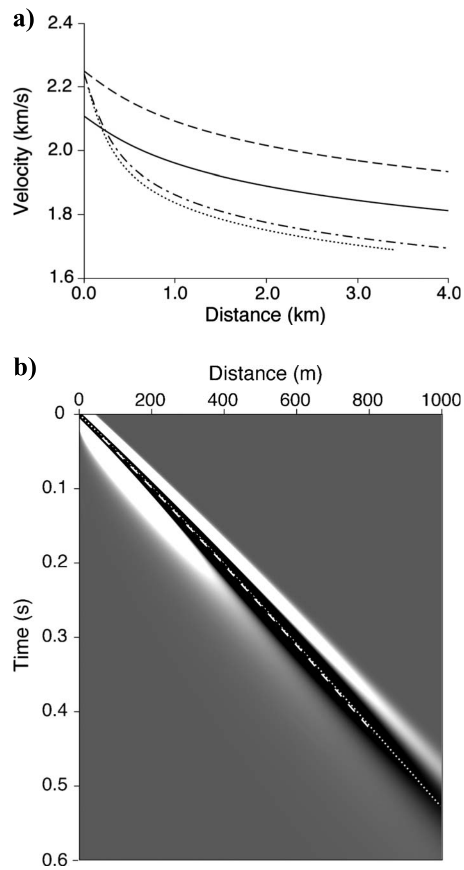

Figure 6. Constant-Q model. (a) The Gurwich (dotted line) and the Smith (dash-dotted line) centrovelocities, and energy and group velocities (solid and dashed lines, respectively) as a function of travel distance; (b) propagating pulse in the space-time domain. The time and space centroids (dotted and dashed line) are computed along the vertical and horizontal directions, respectively. The relaxation mechanism has the peak at $f_0 = 25$ Hz, $Q_0 = 5$, and the source (initial) peak frequency is $f_p = 50$ Hz.

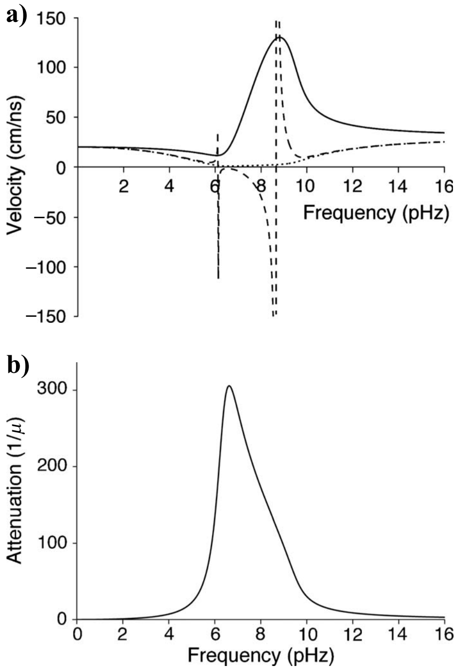

Figure 7. (a) Velocity and (b) attenuation as a function of frequency for the Lorentz model. The solid, dashed, and dotted lines are the energy (phase), Loudon, and group velocities, respectively.

CONCLUSIONS

We have obtained the centrovelocities of different attenuation models as a suitable indication of the location of the pulse, in principle corresponding to the location of the energy. Although for pulses that are not monochromatic (or quasi-monochromatic), the simple concepts of group velocity and energy velocities (obtained from the Umov-Poynting theorem) are approximations; they provide a fairly good indication of the location of the energy for absorbing materials. In particular, the energy velocity performs better than the group velocity in the presence of loss and, in any case, when exceeding a given travel distance.

For the Zener, Debye, and constant-Q models, the group velocity approximates the centrovelocity at short travel distances. At a given distance, the centrovelocity equals the energy velocity, and beyond that distance it becomes a better approximation than the group velocity. However, it is important to note that for electromagnetic media, the group velocity exceeds the velocity of light in vacuum for a certain range of frequencies, whereas the energy velocity is always less than the velocity of light.

For the ionic-conductivity model, the group and energy velocities vanish at the low-frequency limit, and the attenuation factor is constant for nonzero frequencies. Due to this fact, the centrovelocity is nearly constant. In this case, the group velocity also provides a good approximation for the propagation of the localized pulse because this gradually attenuates without changing its shape.

The centrovelocities computed in the time and spatial domains are slightly different, and this difference increases for increasing attenuation. For practical purposes, the two concepts can be considered to be equivalent. It is important to notice that, at least for the constant-Q model, the mean (average) centrovelocities are closer to the energy velocity than the instantaneous Gurwich and Smith centrovelocities.

There are cases when the classical velocities fail. The velocities corresponding to the Lorentz model show anomalous behaviors. The group velocity has singularities and takes negative values, and the classical energy velocity exceeds the velocity of light. On the other hand, the Loudon velocity is well behaved at all frequency ranges.

This analysis is performed in 1D space. All of the concepts can be generalized to the case of extended spatial dimensions, wherein the wavenumber and attenuation vectors do not point in the same direction (wave inhomogeneity). This implies additional attenuation and dispersion effects due to the inhomogeneity angle.

ACKNOWLEDGMENTS

We thank the editors and three anonymous reviewers for their useful comments.

APPENDIX A

ATTENUATION MODELS

Relaxation model

It is well known that the Debye model used to describe the behavior of dielectric materials is mathematically equivalent to the Zener or standard linear solid model used in viscoelasticity to describe a single relaxation peak (e.g., Carcione, 1999). The complex modulus of a Zener element is

$$M(\omega) = M_0\left(\frac{1 + i\omega\tau_\epsilon}{1 + i\omega\tau_\sigma}\right), \tag{A-1}$$

where M_0 is the relaxed modulus,

$$\tau_\sigma = \frac{\tau_0}{Q_0}(\sqrt{Q_0^2 + 1} - 1), \quad \text{and } \tau_\epsilon = \tau_\sigma + \frac{2\tau_0}{Q_0}, \quad (\tau_\epsilon < \tau_\sigma) \tag{A-2}$$

(It is verified that $\tau_0 = \sqrt{\tau_\sigma \tau_\epsilon}$). The quality factor of the Zener model has the minimum value Q_0 at $\omega_0 = 1/\tau_0$.

Equation A-1 can be rewritten as

$$M(\omega) = M_\infty + \frac{M_0 - M_\infty}{1 + i\omega\tau_\sigma}, \tag{A-3}$$

where $M_\infty = M_0 \tau_\epsilon / \tau_\sigma$ is the unrelaxed modulus ($M_\infty > M_0$).

The analogy between the dielectric and viscoelastic models is

$$\begin{aligned} \epsilon_0 &\leftrightarrow M_0^{-1} \\ \epsilon_\infty &\leftrightarrow M_\infty^{-1} \\ \epsilon^* &\leftrightarrow M^{-1} \\ \tau_D &\leftrightarrow \tau_\epsilon \\ \tau_E &\leftrightarrow \tau_\sigma \end{aligned} \tag{A-4}$$

(Carcione, 1999), where ϵ_0 is the static (low-frequency) dielectric permittivity, $\epsilon_\infty = \epsilon_0 \tau_E / \tau_D$ is the optical (high-frequency) dielectric permittivity ($\epsilon_\infty < \epsilon_0$), τ_E and τ_D are relaxation times ($\tau_E < \tau_D$), and

$$\epsilon^*(\omega) = \epsilon_0\left(\frac{1+i\omega\tau_E}{1+i\omega\tau_D}\right), \quad \text{(A-5)}$$

or

$$\epsilon^*(\omega) = \epsilon_\infty + \frac{\epsilon_0-\epsilon_\infty}{1+i\omega\tau_D}. \quad \text{(A-6)}$$

The dielectric permittivity A-6 describes the response of polar molecules, such as water, to the electromagnetic field (Debye, 1929; Turner and Siggins, 1994), and is used to model propagation for ground-penetrating radar applications (Carcione, 1996; Carcione and Schoenberg, 2000). Similar to the viscoelastic case, the relaxation times can be expressed in terms of the minimum quality factor and central frequency of the Debye peak,

$$\tau_E = \left(\frac{\tau_0}{Q_0}\right)(\sqrt{Q_0^2+1}-1) \quad \text{and} \quad \tau_D = \tau_E + \frac{2\tau_0}{Q_0}. \quad \text{(A-7)}$$

It is found that

$$a(\omega) = \frac{2(1-\omega^2\tau_0^2)+i\omega(\tau_\epsilon+3\tau_\sigma)}{2(1+i\omega\tau_\sigma)(1+i\omega\tau_\epsilon)} \quad \text{(A-8)}$$

for the Zener model, and an equivalent expression, according to the correspondence A-4, for the Debye relaxation model (see equation 2).

Ionic-conductivity model

Electromagnetic propagation along the x-axis can be described by Maxwell's equations,

$$\partial_x E_z = \mu\dot{H}_y, \quad -\partial_x H_y = \sigma E_z + \epsilon\dot{E}_z \quad \text{(A-9)}$$

(Wait, 1985), where E_z is the electric field, H_y is the magnetic field, σ is the ionic conductivity, ϵ is the dielectric permittivity, ∂_x is the spatial derivative, and a dot above a variable denotes time differentiation. If the first equation is differentiated with respect to the time variable and the second equation is differentiated with respect to x, combination of the two results and a time Fourier transform gives the Helmholtz equation

$$\partial_{xx}H_y + k^2H_y = 0, \quad \text{(A-10)}$$

where k and v are given by equations 4 and 7, with

$$\epsilon^* = \epsilon - \frac{i\sigma}{\omega}. \quad \text{(A-11)}$$

This electromagnetic model has its viscoelastic equivalent in the Maxwell stress-strain relation (Ben-Menahem and Singh, 1981; Carcione, 2007). The analogy is

$$\epsilon^* \leftrightarrow M^{-1}$$
$$\epsilon \leftrightarrow M_\infty^{-1}$$
$$\sigma \leftrightarrow \eta^{-1} \quad \text{(A-12)}$$

(Carcione and Cavallini, 1995; Carcione and Robinson, 2002), where η is the viscosity of the Maxwell model. The corresponding bulk modulus is

$$M = \frac{\omega\eta}{\omega\tau - i}, \quad \text{(A-13)}$$

where $\tau = \eta/M_\infty$ is a relaxation time.

We obtain, for the ionic-conductivity model,

$$a(\omega) = 1 + \frac{i\sigma}{2\omega\epsilon^*}. \quad \text{(A-14)}$$

Constant-Q model

Constant-Q models provide a good parameterization of seismic attenuation in rocks. Moreover, there is physical evidence that attenuation is almost linear with frequency (therefore Q is constant) in many frequency bands. Bland (1960) and Kjartansson (1979) discuss a linear attenuation model with the required characteristics, but the idea is much older (Scott-Blair, 1949). The complex modulus is given by

$$M(\omega) = M_0\left(\frac{i\omega}{\omega_0}\right)^{2\gamma}, \quad \text{(A-15)}$$

where M_0 is a bulk modulus, γ is a dimensionless parameter, and ω_0 is a reference frequency. The parameter γ quantifies the attenuation

$$\gamma = \frac{1}{\pi}\tan^{-1}\left(\frac{1}{Q_0}\right), \quad \text{(A-16)}$$

where Q_0 is the quality factor. Hence, we see that $Q_0 > 0$ is equivalent to $0 < \gamma < 1/2$. At very high frequencies, the signal propagates at almost infinite velocity, and the differential equation describing the wave motion is parabolic (e.g., Carcione et al., 2002; Carcione, 2007).

For this model, the coefficient a of the group velocity 2 is constant,

$$a = 1 - \gamma. \quad \text{(A-17)}$$

Lorentz model

The theory of resonance attenuation in solid, liquid, and gaseous media is due mainly to Lorentz. The model describes dielectric-type media as a set of neutral atoms with "elastically" bound electrons to the nucleus, where each electron is bound by a Hooke's law restoring force (Nussenzveig, 1972; Oughstun and Sherman, 1994). The atoms vibrate at a resonance frequency under the action of an electromagnetic field. This process implies attenuation because the electrons emit electromagnetic waves, which carry away energy. The classical Lorentz model for a homogeneous dispersive medium has the following complex dielectric permittivity:

$$\epsilon^* = \epsilon^0\left(1 - \frac{b^2}{\omega^2-\omega_0^2-2i\delta\omega}\right) \quad \text{(A-18)}$$

(Born and Wolf, 1964), where ϵ^0 is the free-space dielectric permittivity, b is the plasma frequency of the medium, ω_0 is the resonance frequency, and δ is the associated phenomenological damping constant. A Lorentz medium shows strong attenuation near the absorption line, i.e., near the resonance frequency ω_0.

In this case,

$$a(\omega) = 1 - \frac{\omega(i\delta - \omega)}{b^2}\left(1 - \frac{\epsilon^*}{\epsilon^0}\right)^2 \frac{\epsilon^0}{\epsilon^*}. \quad \text{(A-19)}$$

Loudon (1970) has derived a different expression of the energy velocity, based on the fact that when the frequency of the wave is close to the oscillator frequency ω_0, part of the energy resides in the excited oscillators. This part of the energy must be added to the electromagnetic field energy. The Loudon energy velocity is

$$v_L = \left(\frac{1}{v_e} + \frac{\alpha}{\delta}\right)^{-1} \quad \text{(A-20)}$$

(Oughstun and Sherman, 1994), where v_e and α are given by equations 1 and 5, respectively.

APPENDIX B

ENERGY VELOCITY FOR COMPLEX FREQUENCIES

Let us consider the 1D elastic case and the displacement plane wave

$$u = u_0 \exp[i(\Omega t - \kappa x)], \quad \text{(B-1)}$$

where $\Omega = \omega + i\omega_I$ is the complex frequency, and κ is the real wavenumber. It is clear that the phase velocity is equal to ω/κ.

The balance between the surface and inertial forces is given by

$$\frac{\partial \sigma}{\partial x} = \rho \ddot{u}, \quad \text{(B-2)}$$

here σ is the stress. Because $\sigma = M\epsilon = M\partial u/\partial x$, where ϵ is the strain, we obtain the dispersion relation

$$M\kappa^2 = \rho\Omega^2, \quad \text{(B-3)}$$

which gives the complex velocity

$$v(\kappa) = \frac{\Omega}{\kappa} = \sqrt{\frac{M[\Omega(\kappa)]}{\rho}}. \quad \text{(B-4)}$$

To compute the balance equation for average quantities, we note that

$$-\kappa v^* \sigma = \Omega\rho|v|^2 \quad \text{(B-5)}$$

and

$$-\kappa v^* \sigma = \Omega^* M|\epsilon|^2, \quad \text{(B-6)}$$

where the asterisk indicates complex conjugate. These equations were obtained by multiplying equation B-2 by v^* and $(\partial v/\partial x)^* = \dot{\epsilon}^*$ by σ, respectively.

We introduce the complex Umov-Poynting energy flow

$$p = -\frac{1}{2}\sigma v^*, \quad \text{(B-7)}$$

the time-averaged kinetic-energy density

$$\langle T\rangle = \frac{1}{2}\langle\rho[\mathrm{Re}(v)]^2\rangle = \frac{1}{4}\rho\,\mathrm{Re}(vv^*) = \frac{1}{4}\rho|v|^2, \quad \text{(B-8)}$$

the time-averaged strain-energy density

$$\langle V\rangle = \frac{1}{2}\langle\mathrm{Re}(\epsilon)\mathrm{Re}(M)\mathrm{Re}(\epsilon)\rangle = \frac{1}{4}\,\mathrm{Re}(\epsilon M\epsilon^*) = \frac{1}{4}\,\mathrm{Re}(M) \times|\epsilon|^2, \quad \text{(B-9)}$$

and the time-averaged dissipated-energy density

$$\langle D\rangle = \langle\mathrm{Re}(\epsilon)\mathrm{Im}(M)\mathrm{Re}(\epsilon)\rangle = \frac{1}{2}\,\mathrm{Im}(\epsilon M\epsilon^*) = \frac{1}{2}\,\mathrm{Im}(M)|\epsilon|^2. \quad \text{(B-10)}$$

Thus, in terms of the energy flow and energy densities, equations B-5 and B-6 become

$$\frac{\kappa p}{\Omega} = 2\langle T\rangle \quad \text{(B-11)}$$

and

$$\frac{\kappa p}{\Omega^*} = 2\langle V\rangle + i\langle D\rangle. \quad \text{(B-12)}$$

Adding equations B-11 and B-12, we have

$$2\kappa p\,\mathrm{Re}\left(\frac{1}{\Omega}\right) = 2\omega\langle E\rangle + i\langle D\rangle, \quad \text{(B-13)}$$

where

$$\langle E\rangle = \langle T + V\rangle \quad \text{(B-14)}$$

is the time-averaged energy density.

Separating equation B-13 into real and imaginary parts, and using the concept that

$$\langle p\rangle = \mathrm{Re}(p) \quad \text{(B-15)}$$

is the time-averaged power-flow density, the energy velocity is given by

$$v_e = \frac{\langle p\rangle}{\langle E\rangle} = \left[\kappa\,\mathrm{Re}\left(\frac{1}{\Omega}\right)\right]^{-1} = \left[\mathrm{Re}\left(\frac{1}{v}\right)\right]^{-1}; \quad \text{(B-16)}$$

i.e., the energy velocity has the same expression as a function of the complex velocity, no matter if the frequency is complex or the wavenumber is complex. On the contrary, the phase velocity is given by equation B-16 for real frequencies, and it is equal to Re(v) for real wavenumbers and complex frequencies.

REFERENCES

Ben-Menahem, A., and S. J. Singh, 1981, Seismic waves and sources: Springer-Verlag.
Bland, D. R., 1960, The theory of linear viscoelasticity: Pergamon Press.
Bloch, S. C., 1977, Eighth velocity of light: American Journal of Physics, **45**, 538–549.
Borcherdt, R. D., 1973, Energy and plane waves in linear viscoelastic media: Journal of Geophysical Research, **78**, 2442–2453.
Born, M., and E. Wolf, 1964, Principles of optics: Pergamon Press.
Bracewell, R., 1965, The Fourier transform and its applications: McGraw-Hill Book Co.
Brillouin, L., 1960, Wave propagation and group velocity: Academic Press.
Buchen, P. W., 1971, Plane waves in linear viscoelastic media: Geophysical Journal of the Royal Astronomical Society, **23**, 531–542.
Carcione, J. M., 1994, Wavefronts in dissipative anisotropic media: Geo-

physics, **59**, 644–657.
———, 1996, Ground-penetrating radar: Wave theory and numerical simulations in lossy anisotropic media: Geophysics, **61**, 1664–1677.
———, 1999, On energy definition in electromagnetism: An analogy with viscoelasticity: Journal of the Acoustical Society of America, **105**, no. 2, 626–632.
———, 2007, Wave fields in real media: Theory and numerical simulation of wave propagation in anisotropic, anelastic, porous and electromagnetic media: Elsevier Science.
Carcione, J. M., and F. Cavallini, 1995, On the acoustic-electromagnetic analogy: Wave Motion, **21**, 149–162.
Carcione, J. M., F. Cavallini, F. Mainardi, and A. Hanyga, 2002, Time-domain seismic modeling of constant Q-wave propagation using fractional derivatives: Pure and Applied Geophysics, **159**, no. 7, 1719–1736.
Carcione, J. M., G. Quiroga-Goode, and F. Cavallini, 1996, Wavefronts in dissipative anisotropic media: Comparison of the plane wave theory with numerical modeling: Geophysics, **61**, 857–861.
Carcione, J. M., and E. Robinson, 2002, On the acoustic-electromagnetic analogy for the reflection-refraction problem: Studia Geophysica et Geodaetica, **46**, 321–345.
Carcione, J. M., and M. Schoenberg, 2000, 3-D ground-penetrating radar simulation and plane wave theory: Geophysics, **65**, 1527–1541.
Chiao, R. Y., 1993, Superluminal (but causal) propagation of wave packets in transparent media with inverted atomic populations: Physical Review A, **48**, no. 1, 34–37.
Daniels, D. J., 1996, Surface-penetrating radar: The Institution of Electrical Engineers Radar, Sonar, Navigation and Avionics Series No. 6.
Debye, P., 1929, Polar molecules: Dover Publications.
Derks, G., and E. van Groesen, 1992, Energy propagation in dissipative systems: Part 2 — Centrovelocity for nonlinear systems: Wave Motion, **15**, 159–172.
Eckart, C., 1948, The approximate solution of one-dimensional wave equations: Reviews of Modern Physics, **20**, 399–417.
Felsen, L. P., and N. Marcuvitz, 1973, Radiation and scattering of waves: Prentice-Hall.
Garrett, C. G. B., and D. E. McCumber, 1970, Propagation of a Gaussian light pulse through an anomalous dispersion medium: Physical Review A, **1**, no. 2, 305–313.
Gurwich, I., 2001, On the pulse velocity in absorbing and non-linear media and parallels with the quantum mechanics: Progress in Electromagnetics Research, **33**, 69–96.
Kjartansson, E., 1979, Constant Q-wave propagation and attenuation: Journal of Geophysical Research, **84**, 4737–4748.
Loudon, R., 1970, The propagation of electromagnetic energy through an absorbing medium: Journal of Physics A, **3**, 233–245.
Mainardi, F., 1973, On energy velocity of viscoelastic waves: Lettere al Nuovo Cimento, **6**, 443–449.
———, 1983, Signal velocity for transient waves in linear dissipative media: Wave Motion, **5**, 33–41.
———, 1987, Energy velocity for hyperbolic dispersive waves: Wave Motion, **9**, 201–208.
Nussenzveig, H. M., 1972, Causality and dispersion relations: Academic Press.
Oughstun, K. E., and G. C. Sherman, 1994, Electromagnetic pulse propagation in causal dielectrics: Springer-Verlag.
Postma, G. W., 1955, Wave propagation in a stratified medium: Geophysics, **20**, 780–806.
Scott-Blair, G. W., 1949, Survey of general and applied rheology: Pitman.
Smith, R. L., 1970, The velocity of light: American Journal of Physics, **38**, 978–984.
Steinberg, A. M., and R. Y. Chiao, 1994, Dispersionless, highly superluminal propagation in a medium with a gain doublet: Physical Review A, **49**, no. 3, 2071–2075.
Turner, G., and A. F. Siggins, 1994, Constant-Q attenuation of subsurface radar pulses: Geophysics, **59**, 1192–1200.
Vainshtein, L. A., 1957, Group velocity of damped waves: Soviet Physics — Technical Physics, **2**, 2420–2428.
Van Groesen, E., and F. Mainardi, 1989, Energy propagation in dissipative systems: Part 1 — Centrovelocity for linear systems: Wave Motion, **11**, 201–209.
Wait, J. R., 1985, Electromagnetic wave theory: Harper and Row.
Wang, L. J., A. Kuzmich, and A. Dogariu, 2000, Gain-assisted superluminal light propagation: Nature, **406**, 277–279.